BMC Nephrology

RESEARCH

Open Access

Glycolytic control proteins in urinary extracellular vesicles are elevated during kidney transplant T cell-mediated rejection

P.Y.M. Leung[1,2*], A.S. Graver[1,2,3], M. Katerelos[2], A. Skene[4], J.B. Whitlam[1,2,3], D.A. Power[1,2] and P.F. Mount[1,2]

Abstract

Background A priority in kidney transplant management is the ability to monitor allograft health accurately, frequently and less-invasively. Metabolic reprogramming from fatty acid oxidation to glycolysis has been associated with kidney injury. Given the histological localisation of T cell-mediated rejection (TCMR) to the tubulointerstitium, we hypothesised that expression of glycolytic control proteins contained in urinary extracellular vesicles (UEV) may increase during TCMR.

Methods In this prospective observational study, urine samples were collected from kidney transplant recipients prior to indication biopsy. UEV were separated by differential ultracentrifugation. Vesicle markers, glycolytic control proteins and CD3 were assayed by immunoblotting. Differences in protein detection were compared across biopsy diagnoses (TCMR versus not) and Banff lesion scores.

Results 51 paired urine and biopsy samples from 43 subjects were included. The TCMR group comprised of 6 cases of TCMR and 1 borderline TCMR. The remaining 44 samples comprised a "No TCMR" group. There was significant increase in phosphofructo-2-kinase/fructose-2,6-bisphosphatase 4 (PFKFB4) ($p=0.018$) in TCMR compared to No TCMR, and similarly when tubulitis ($p=0.037$) and interstitial inflammation ($p=0.047$) were present. Total inflammation score ≥ 1 was associated with increases in PFKFB2 ($p=0.027$), PFKFB3 ($p=0.090$) and PFKFB4 ($p=0.0098$). Interstitial fibrosis was associated with increased PFKFB2 ($p=0.0045$) and PFKFB3 ($p=0.045$). CD3 + UEV did not correlate with TCMR diagnosis. When combining the four glycolytic control proteins governing the phosphofructokinase-1 step of glycolysis (PFK-L, PFKFB2, PFKFB3 and PFKFB4), presence of ≥ 3 markers discriminated TCMR with ROC AUC of 0.73 (95% CI 0.50–0.96).

Conclusion Increased rate-limiting enzymes of glycolysis in UEV were detected in association with tubulointerstitial inflammation and fibrosis. This suggests altered energy metabolism in the form of increased renal glycolysis occurring in the tubular epithelium, consistent with findings in native kidney injury. Further work is required to evaluate whether this could serve as a non-invasive strategy to study pathology in kidney transplantation.

Keywords Glycolytic control proteins, Kidney transplant, T cell-mediated rejection, Urinary extracellular vesicles

*Correspondence:
P.Y.M. Leung
mia.leung@austin.org.au
[1]Faculty of Medicine, Dentistry and Health Sciences, University of Melbourne, Melbourne, Parkville, Australia
[2]Department of Nephrology, Austin Health, 145 Studley Road, Heidelberg, Melbourne VIC 3084, Australia
[3]Australian Centre for Transplantation Excellence and Research, Austin Health, Melbourne, Australia
[4]Department of Anatomical Pathology, Austin Health, Melbourne, Australia

Background

Experimental evidence has associated kidney injury with changes in kidney energy metabolism, but the metabolic changes during kidney transplant rejection are not well understood [1–3]. Tubular cells along the nephron generate energy from various substrates in order to maintain complex homeostatic functions [4]. However, metabolic preference is not uniform and depends on the cell type. The proximal tubule derives adenosine triphosphate (ATP) from mitochondrial oxidative phosphorylation of fatty acids and has limited capacity to perform glycolysis [4]. By contrast, distal segments preferentially utilise glycolysis due to low oxygen tension in the inner medulla [4].

Glycolysis is a series of ten chemical reactions that metabolise glucose to pyruvate with the net release of two ATP molecules [5, 6]. There are three rate-limiting enzymes– hexokinase, phosphofructokinase-1 (PFK-1) and pyruvate kinase (PK) [7]. Hexokinase catalyses the first step of glycolysis to trap glucose inside the cell [3]. PFK-1 catalyses the ATP-dependent conversion of fructose-6-phosphate to fructose-1,6-bisphosphate, promoting the forward reaction of glycolysis [8]. Phosphofructokinase-liver (PFK-L) is the dominant isoform of PFK-1 in the kidney [9]. The most potent activator of PFK-1 is the level of fructose-2,6-bisphosphate, which is controlled by a family of enzymes with bifunctional actions, called 6-phosphofructo-2-kinase/fructose-2,6-bisphosphatases (PFKFB) [10]. The four isoenzymes PFKFB1-4 differ in relative kinase:phosphatase ratios. They also differ in tissue distribution and specifically regulate the formation and degradation of fructose-2,6-bisphosphate in response to cellular requirements [11]. PFKFB1 is not expressed in the kidney, whereas PFKFB2-4 are distributed throughout the nephron [12]. Pyruvate kinase catalyses the last step of glycolysis to form pyruvate. In aerobic conditions, pyruvate enters the mitochondria and undergoes oxidative phosphorylation. In the anaerobic state, it is converted to lactate [4]. Aerobic glycolysis (the conversion of pyruvate to lactate under normoxic condition) can occur as an adaptive or pathological response [13].

Conventional monitoring of kidney allograft function relies on serial measurements of serum creatinine, urine protein and biopsies [14]. These methods have low sensitivity and specificity for rejection [15]. Early detection and treatment of rejection is a key priority in post-transplant management [16], prompting evaluation of novel biomarkers to support this.

Urinary extracellular vesicles (UEV) are a source of potential biomarkers. These are nano-sized particles released from cells lining the kidney and urinary tract, which contain distinctive cargo from their parent cells [17]. The protein compartment has been shown to closely reflect changes occurring in kidney cells, in particular proteins restricted to the renal tubule [18]. An increasing number of physiological roles have been ascribed to UEV, including immunomodulation, transfer of cargo and mediation of cell-cell communication [19].

The histological hallmarks of T cell-mediated rejection (TCMR) are tubulitis and interstitial inflammation, with or without arteritis [20]. We hypothesised that TCMR is associated with metabolic stress and a shift to increased glycolysis, which may be detectable by increased expression of glycolytic control proteins in UEV, given the pathophysiological changes occurring in tubular epithelium contiguous to the urinary space. In this clinical proof-of-principle study, we aimed to determine whether there are changes in glycolytic control proteins contained in the UEV of kidney transplant recipients undergoing allograft biopsy for clinical indications. Variations in glycolytic control proteins were correlated to histologic diagnosis of TCMR and individual Banff lesions.

Methods

This prospective, cross-sectional study was approved by the institutional Human Research Ethics Committee (HREC/58942/Austin-2019) and written informed consent was obtained from participants. Adult kidney transplant recipients (age > 18 years) undergoing an indication biopsy were asked to provide 50 mL of urine prior to biopsy. Indication biopsies were determined by treating clinician to investigate acute graft dysfunction due to creatinine rise, proteinuria, or both. Biopsies performed by protocol or for follow up of rejection episode were not included. Excluded were recipients within two weeks post-transplant due to expected dynamic changes in urine composition and graft function, and recipients of multi-organ transplantation.

Recommendations from International Society of Extracellular Vesicles were followed including reporting of pre-analytical parameters, isolation and protein characterisation of UEV [19, 21]. The urine sample was centrifuged at 1,600xg at 4˚C for 10 minutes to remove cellular debris (Megafuge 1.0 R, Heraeus). Supernatant was divided into 10 mL aliquots with 100 µL protease inhibitor 400 µg/mL (PI, Sigma-Aldrich protease inhibitor cocktail P8340, Missouri, USA) and then stored at – 80˚C until required.

Separation of UEV was by differential ultracentrifugation as described by Wolley et al. [22]. In brief, 10 mL of frozen urine was vortexed vigorously until thawed, aliquoted into three 3 mL Beckman polycarbonate tubes, then centrifuged at 17,000 x g at 4˚C for 15 minutes (Optima TLX 120CE ultracentrifuge, Beckman Coulter, Inc). The supernatant was incubated with dithiothreitol (DTT, Bio-Rad Laboratories Pty Ltd, NSW, Australia) at a final concentration of 8.3 mg/mL for 10 minutes at

37˚C. The sample was aliquoted into three new polycarbonate tubes then ultracentrifuged at 200,000 x g at 4˚C for 60 minutes to pellet the UEV. The supernatant was discarded, and the pellets were resuspended with 500 µL PBS/PI/DTT solution (125 µL DTT and 125 µL PI in 10 mL phosphate buffered saline). The tubes were vortexed for 30 seconds and the samples were pooled into one new polycarbonate tube. This step was repeated to resuspend pellets again in a final volume of 3 mL. This sample underwent a second ultracentrifugation at 200,000 x g at 4˚C for 60 minutes. The supernatant was discarded, and the pellet was resuspended in 41 µL PBS/PI/DTT solution and vortexed for 30 seconds. Subsequently, 40 µL was placed into an Eppendorf tube, and 10 µL SDS sample buffer was added to denature proteins for Western blot analysis. The final sample was vortexed for 30 seconds and 20 µL was aliquoted into a new Eppendorf tube. This was incubated at 60˚C for 10 minutes and then stored at – 80˚C until use.

Particle size and concentration was assessed by nanoparticle tracking analysis (NTA) in a representative sample of four healthy individuals. After differential ultracentrifugation, 10 µL from the final UEV pellet was diluted in 40 µL phosphate buffered saline (PBS), then stored at – 80 °C for NTA. This was conducted using NanoSight NS300 (Malvern Instruments, UK) equipped with a 488 nm laser. At the time of NTA, PBS was added to the sample resulting in a final dilution of 1:50. The Brownian motion of particles was recorded with five videos of 30 seconds duration, and particle size was calculated using the Stokes-Einstein equation using machine software (NTA 3.2 Dev Build 3.2.16).

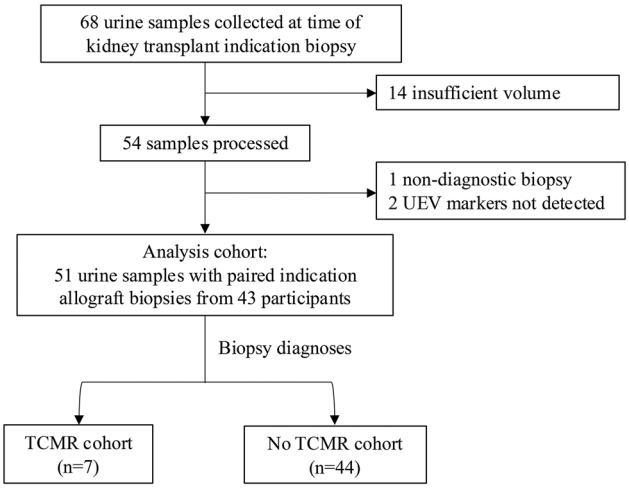

Fig. 1 Flow chart of sample inclusion in the final analysis cohort. Participants were recruited over a 2.5-year period. The final analysis cohort included 51 urine samples with paired indication allograft biopsy samples from 43 participants. These were grouped according to biopsy diagnosis into TCMR (n = 7) or No TCMR (n = 44) groups. UEV, urinary extracellular vesicles; TCMR, T cell-mediated rejection

All proteins were assayed by immunoblotting as previously described [23]. The panel of glycolytic control proteins was determined by reviewing proteomic databases of urinary exosomes (http://www.exocarta.org and http://microvesicles.org) on 18 August 2021 [18]. Hexokinase was not found in urinary exosomes and therefore not included in this study [24]. Primary antibodies were sourced from commercial suppliers (Table S1), including PFK-L, PFKFB2, PFKFB3, PFKFB4, pyruvate kinase-L/R (PK-L/R), pyruvate kinase-M2 (PK-M2), and T cell marker, CD3. UEV markers, CD9 and tumour susceptibility gene 101 (TSG101), and a negative marker, uromodulin, were used to characterise vesicles [21]. At the time of immunoblotting, sample aliquots of 20 µL were loaded into a 10-well 4–15% precast polyacrylamide gel, including Precision Plus prestained protein standard, and positive controls of ischaemic human kidney lysate and peripheral blood mononuclear cells. Protein bands were recorded as present or absent.

Indication allograft biopsies were performed according to local practice. Histopathologic examination was undertaken by blinded pathologists. Using the Banff 2022 schema, study participants were classified into TCMR group based on diagnosis of TCMR or borderline TCMR [20]. Other diagnoses were included in No TCMR group.

Statistical analyses were performed using GraphPad Prism v10.0.3 and R v4.3.1. For the demographic data, continuous variables were compared using unpaired t tests and Fisher's exact test, as appropriate. The percentage of samples where bands were present or absent was analysed using contingency tables and Fisher's exact test. A p-value < 0.05 was considered significant. Receiver operator characteristic area under the curves (ROC AUC) were calculated to assess the diagnostic performance of glycolytic control proteins, creatinine and Δcreatinine, defined as the difference in serum creatinine at the time of indication biopsy and at baseline. Correlated ROC AUCs were compared using the DeLong method [25].

Results

Study cohort

Participants were recruited from February 2021 to August 2023. Fourteen urine samples had insufficient volume. Three samples were excluded due to non-diagnostic biopsy with no glomeruli sampled (n = 1) or absent UEV markers (n = 2). Therefore, 51 samples from 43 participants were included in the final analysis cohort (Fig. 1). Eight participants underwent two indication biopsies during the study period. The TCMR group (n = 7) included 6 TCMR and 1 borderline TCMR cases, whilst the No TCMR group (n = 44) comprised 33 cases with normal biopsy or non-specific changes, 7

antibody-mediated changes, 1 calcineurin inhibitor toxicity and 3 recurrent glomerulonephritis.

Technical validation of the differential ultracentrifugation protocol was undertaken using urine samples from four healthy volunteers. Post-separation characterisation of UEV by immunoblotting confirmed detection of positive markers CD9 and/or TSG101 in three out of four samples (Figure S1a). Using NTA, we measured particle diameter to be < 200 nm, consistent with small extracellular vesicles [26], and particle concentration ranging from 36.6–204.5 × 10^8 particle/mL (Figure S1a, S1b).

Participant characteristics are presented in Table 1. Median age was 54 years (inter-quartile range, IQR, 47–61) and 31% were female. Median time post-transplant was 1.8 years (IQR0.3–9.8). Most participants (86%) had received their first kidney transplant and 63% were from deceased donors. Participants received basiliximab induction immunosuppression in majority of cases (78%) and were maintained on prednisolone, mycophenolate and tacrolimus. Donor age and time between kidney transplantation to biopsy was similar in both groups. There were no significant differences in baseline demographics between groups.

The predominant clinical indication for biopsy was change in serum creatinine (67%), followed by creatinine rise with proteinuria (20%), then isolated proteinuria (14%). Median serum creatinine at baseline was 130 µmol/L (IQR103-160), defined as pre-biopsy creatinine when the participant was clinically stable and without systemic or allograft-related illnesses, and 164 µmol/L (IQR130-214) at the time of biopsy. Median urine protein-creatinine ratio at baseline was 27 mg/mmol (IQR19-77), compared to 33 mg/mmol (16–98) at the time of biopsy.

Urine was collected prior to biopsy in 80% of cases and the remaining samples were collected prior to commencement of rejection treatment. Samples were processed at median 80 minutes following collection (IQR60-120); there was no significant difference between the two groups (p = 0.58).

Immunoblots

By comparing glycolytic control proteins in TCMR versus No TCMR, we detected increased PFKFB4 + UEV in 5/7 (71%) TCMR samples compared to 10/44 (23%) of No TCMR samples (p = 0.018) (Table 2). There were no significant changes in remainder of glycolytic control proteins (Table 2). CD3 was detected in 29% of TCMR cases, compared to 11% of No TCMR cases, which was not statistically different (p = 0.24).

We proceeded to analyse the detection of glycolytic control proteins according to either presence (score ≥ 1) or absence (score = 0) of individual Banff lesions. A representative panel of Western blots of UEV markers, glycolytic control proteins and CD3 according to tubulitis score is presented in Fig. 2. PFKFB4 expression was similarly increased in samples with tubulitis (p = 0.037) and interstitial inflammation (p = 0.047) (Table 3). The presence of v (intimal arteritis) lesion was not associated with altered glycolytic control protein expression (Table 3). Expression of PFKFB2 (p = 0.0045) was increased with i–IFTA (inflammation in areas of interstitial fibrosis and tubular atrophy) (Table 4). Co-expression of PFKFB2 (p = 0.0045) and PFKFB3 (p = 0.045) was detected in biopsies with interstitial fibrosis (Table 4) but not in the setting of tubular atrophy (Table S2). Total inflammation (ti) score was strongly associated with increased PFKFB2 (p = 0.027), PFKFB3 (p = 0.0090) and PFKFB4 (p = 0.0098) (Table 4).

There were no significant differences in glycolytic control proteins in Banff lesions diagnostic of antibody-mediated rejection, including ptc (peritubular capillaritis), g (glomerulitis), C4d (C4d staining) and cg (transplant glomerulopathy) (Tables S5, S6, S7, S8). Analysis of remaining Banff lesions revealed PK-M2 elevation in association with cv (arterial intimal thickening) and ah (arteriolar hyalinosis) (p = 0.040 and 0.037 respectively) (Tables S3 and S4). Additionally, ah ≥ 1 was associated with elevation of PFKFB3 (p = 0.036) (Table S4).

We reviewed individual TCMR cases to understand the profile of glycolytic control proteins (Fig. 3). Those who had positive glycolytic markers frequently had multiple markers detected. Four of 7 (57%) TCMR cases had 4 to 6 glycolytic control proteins detected. This did not clearly relate to the severity of Banff lesions or other clinical characteristics. By contrast, only 5/44 (11%) cases in the No TCMR group had 4 to 6 glycolytic markers detected (p = 0.014). The histological diagnoses in these cases were borderline TCMR (n = 2), severe chronic parenchymal damage, moderate scarring and normal biopsy.

The PFKFB enzymes regulate PFK-1 which controls a key rate-limiting step of glycolysis. Therefore, we selectively analysed these four proteins (PFK-L, PFKFB2, PFKFB3 and PFKFB4) as a panel, instead of individually, to determine whether this could be useful in discriminating TCMR from No TCMR. The ROC AUC was 0.73 (95% CI 0.50–0.96) (Fig. 3). By contrast, ROC AUC for creatinine was 0.62 (95% CI 0.43–0.81) and for Δcreatinine was 0.60 (95% CI 0.34–0.86). The panel of glycolytic control proteins did not perform better when compared to creatinine (AUC 0.73 vs 0.62, Z = 1.03, p = 0.31) and Δcreatinine (AUC 0.73 vs 0.60, Z = 1.31, p = 0.19). Using a threshold of ≥ 3 glycolytic control proteins, this detected TCMR with 57% sensitivity (95% CI 25–84) and 91% specificity (95% CI 79–96). The positive predictive value was 50% (95% CI 22–78) and negative predictive value was 93% (95% CI 81–98), in this cohort with a TCMR prevalence of 14% (Table S9).

Table 1 Baseline participant and transplant characteristics in the total cohort, T cell-mediated rejection (TCMR) and No TCMR groups

	Total cohort (n = 51)	**TCMR (n = 7)**	**No TCMR (n = 44)**	**p-value**
	Participant characteristics			
Age (years)	54 (47–61)	51 (41–60)	55 (47–63)	0.38
Sex	16 (31%)	4 (57%)	12 (27%)	0.11
Female	35 (69%)	3 (43%)	32 (73%)	
Male				
Primary kidney disease	24 (47%)	2 (28%)	22 (50%)	0.37
Glomerulonephritis	5 (10%)	1 (14%)	4 (9%)	
Hypertension	5 (10%)	2 (28%)	3 (7%)	
Reflux nephropathy	4 (8%)	0 (0%)	4 (9%)	
Diabetic nephropathy	3 (6%)	0 (0%)	3 (7%)	
FSGS	10 (20%)	2 (28%)	8 (18%)	
Other				
Years between transplantation and biopsy	1.8 (0.33–9.8)	2.1 (0.67–9.8)	1.2 (0.33–9.5)	0.87
Body mass index (kg/m^2)	26.9 (24.4–34.7)	28.3 (26.0–36.7)	26.9 (24.1–32.1)	0.30
	Transplant characteristics			
Graft number	44 (86%)	6 (86%)	38 (86%)	>0.99
First	6 (12%)	1 (14%)	5 (11%)	
Second	1 (2%)	0 (0%)	1 (2%)	
Third				
Donor type	32 (63%)	5 (71%)	27 (61%)	0.70
Deceased donor	19 (37%)	2 (29%)	17 (39%)	
Living donor				
Donor age	52 (52–60)	57 (45–62)	51 (39–60)	0.52
ABO incompatible	6 (12%)	1 (14%)	5 (12%)	>0.99
DSA at transplant	8 (16%)	1 (14%)	7 (17%)	>0.99
HLA mismatch	10 (20%)	3 (43%)	7 (16%)	0.20
5–6	17 (34%)	1 (14%)	16 (36%)	
3-4	23 (46%)	3 (43%)	20 (45%)	
1–2	0 (0%)	0 (0%)	0 (0%)	
0				
Induction agent	40 (78%)	5 (71%)	35 (80%)	0.67
Basiliximab	1 (2%)	0 (0%)	1 (2%)	
rATG	10 (20%)	2 (29%)	8 (18%)	
Unknown				
Maintenance immunosuppression	50 (98%)	7 (100%)	43 (98%)	>0.99
Prednisolone	46 (90%)	6 (86%)	40 (91%)	0.54
Mycophenolate	1 (2%)	0 (0%)	1 (2%)	>0.99
Azathioprine	47 (92%)	7 (100%)	40 (91%)	>0.99
Tacrolimus	4 (8%)	0 (0%)	4 (9%)	>0.99
Cyclosporin	2 (4%)	1 (14%)	1 (2%)	0.26
mTOR				
	Sample characteristics			
Biopsy indication	34 (67%)	6 (86%)	28 (64%)	0.71
Creatinine rise	8 (14%)	0 (0%)	8 (18%)	
Proteinuria	9 (20%)	1 (14%)	8 (18%)	
Both				
Serum creatinine (μmol/L)	130 (103–160)	143 (122–161)	123 (101–159)	0.95
Baseline	164 (130–214)	168 (157–241)	158 (125–212)	0.70
At time of biopsy				
Urine PCR (mg/mmol)	27 (19–77)	29 (18–50)	26 (19–84)	0.38
Baseline	33 (16–98)	131 (8–284)	33 (16–98)	0.53
At time of biopsy				
Tacrolimus level (ug/L)	5.5 (4.5–6.9)	4.7 (4.1–6.0)	5.6 (4.7–6.9)	0.20

Continuous variables are presented as median (inter-quartile range) and differences between two groups were compared using unpaired t test. Categorical variables were analysed by Fisher's exact test and presented as number (%). Missing data in donor age (n = 50), ABO incompatible (n = 50), DSA at transplant (n = 49), HLA mismatch (n = 50), urine protein-creatinine ratio at baseline (n = 40), urine protein-creatinine ratio at time of biopsy (n = 39) and tacrolimus level (n = 44). Serum creatinine at baseline not available for one participant as baseline not yet established post-transplant (n = 50). FSGS, focal segmental glomerulosclerosis; DSA, donor-specific antibody; HLA, human leucocyte antigen; rATG, rabbit anti-thymocyte globulin; mTOR, mammalian target of Rapamycin; urine PCR, urine protein-creatinine ratio

Table 2 Detection of glycolytic control proteins and CD3 in TCMR and No TCMR cohorts

	TCMR (n = 7)	No TCMR (n = 44)	p-value
PFK-L	3 (43%)	7 (16%)	0.13
PFKFB2	4 (57%)	12 (27%)	0.19
PFKFB3	3 (43%)	6 (14%)	0.095
PFKFB4	**5 (71%)**	**10 (23%)**	**0.018***
PK-L/R	1 (14%)	4 (9%)	0.54
PK-M2	6 (86%)	30 (68%)	0.66
CD3	2 (29%)	5 (11%)	0.24

Contingency table and Fisher's exact test were used to compare the two groups

Discussion

To our knowledge, this is the first study to focus on urine biomarkers of energy metabolism in kidney transplant rejection. In contrast to unbiased proteomic evaluation of UEV which detected various candidate biomarkers [27–31], this directed approach incorporates the existing understanding of kidney energy metabolism [3].

A key finding of this study is increased PFKFB4 + UEV in association with TCMR compared to No TCMR. When analysing Banff lesions diagnostic of TCMR, PFKFB4 + UEV was consistently increased when tubulitis and interstitial inflammation was present. This raises the possibility that altered energy metabolism in the form of increased renal glycolysis is occurring in tubular epithelium during TCMR.

Elevations of PFKFB enzymes in various combinations, was observed in association with tubulointerstitial inflammation and fibrosis. I–IFTA, which can represent a transitional lesion of T cell-mediated acute inflammation to fibrosis [32], was associated with elevation of PFKFB2 + UEV. Another important observation was the strong association of the ti score, which encompasses inflammation in the scarred and non-scarred cortex [33], with the greatest number of glycolytic control

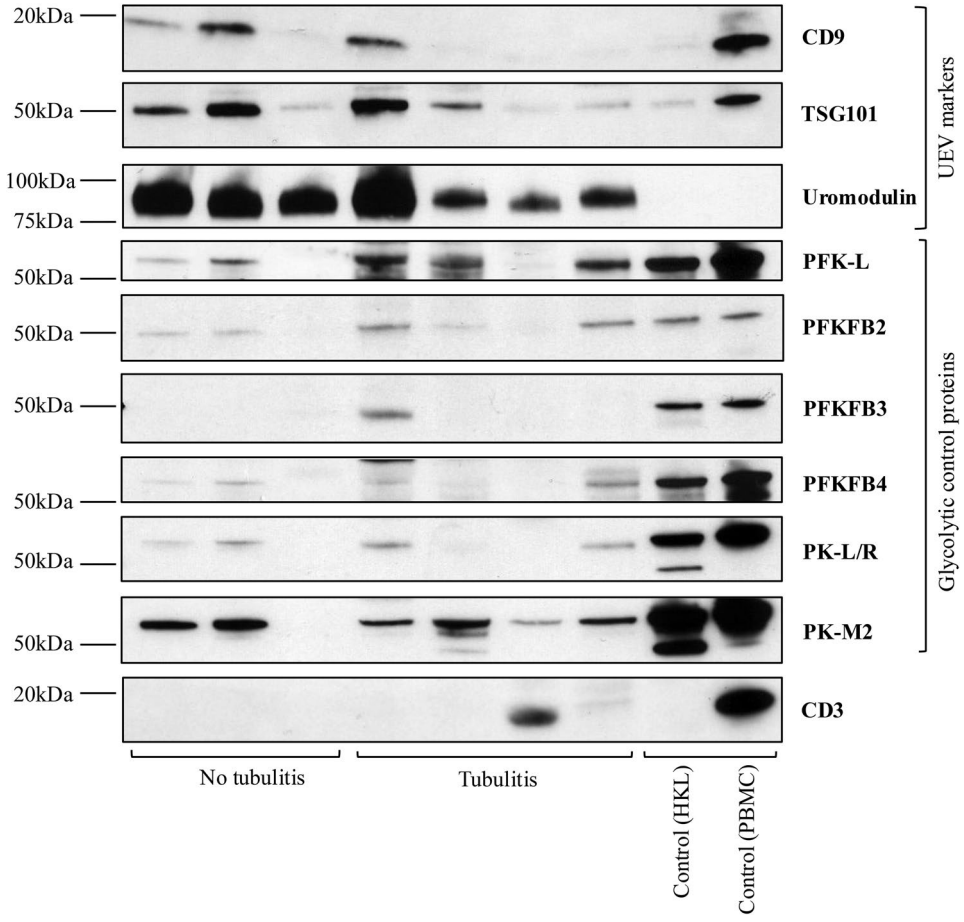

Fig. 2 Representative Western blots of vesicle markers, glycolytic control proteins and CD3 in UEV of participants with no tubulitis (n = 3) and tubulitis (n = 4) and positive controls. Each lane represents an individual urine sample from an individual patient. Uncropped blots are presented in Supplementary Materials. UEV, urinary extracellular vesicles; PFK-L, phosphofructokinase-liver; PFKFB2, phosphofructo-2-kinase/fructose-2,6-bisphosphatase 2; PFKFB3, phosphofructo-2-kinase/fructose-2,6-bisphosphatase 3; PFKFB4, phosphofructo-2-kinase/fructose-2,6-bisphosphatase 4; PK-L/R, pyruvate kinase-L/R; PK-M2, pyruvate kinase-M2; HKL, human kidney lysate; PBMC, peripheral blood mononuclear cell

Table 3 Number of bands present (%) on Western blot of glycolytic control proteins in UEV based on renal biopsy tubulitis (t), interstitial inflammation (i) and intimal arteritis (v) scores on Banff criteria

	Tubulitis (t)			Interstitial inflammation (i)			Intimal arteritis (v)		
Score	**0**	**≥ 1**	**p-value**	**0**	**≥ 1**	**p-value**	**0**	**≥ 1**	**p-value**
n	**38**	**13**		**41**	**10**		**46**	**4**	
PFK-L	5 (13%)	5 (38%)	0.099	7 (17%)	3 (30%)	0.39	9 (20%)	1 (25%)	>0.99
PFKFB2	10 (26%)	6 (46%)	0.30	12 (29%)	4 (40%)	0.71	15 (31%)	1 (25%)	>0.99
PFKFB3	5 (13%)	4 (31%)	0.21	5 (12%)	4 (40%)	0.061	7 (15%)	1 (25%)	0.51
PFKFB4	**8 (21%)**	**7 (54%)**	**0.037***	**9 (22%)**	**6 (60%)**	**0.047***	12 (26%)	2 (50%)	0.31
PK-L/R	3 (8%)	2 (15%)	0.59	4 (10%)	1 (10%)	>0.99	4 (9%)	1 (25%)	0.35
–	27 (71%)	9 (69%)	>0.99	27 (66%)	9 (90%)	0.25	33 (72%)	2 (50%)	0.57
CD3	5 (13%)	2 (15%)	>0.99	5 (12%)	2 (20%)	0.61	6 (13%)	1 (25%)	0.46

Comparison made using contingency tables and Fisher's exact test. Missing data in one participant for intimal arteritis (v) score as arteries not represented in biopsy sample

Table 4 Number of bands present (%) on Western blot of glycolytic control proteins in UEV based on renal biopsy inflammation in areas of interstitial fibrosis and tubular atrophy (i–IFTA), interstitial fibrosis (ci) and total inflammation (ti) scores on Banff criteria

	Inflammation in areas of interstitial fibrosis and tubular atrophy (i–IFTA)			Interstitial fibrosis (ci)			Total inflammation (ti)		
Score	**0**	**≥ 1**	**p-value**	**0**	**≥ 1**	**p-value**	**0**	**≥ 1**	**p-value**
n	**34**	**17**		**34**	**17**		**32**	**19**	
PFK-L	4 (12%)	6 (35%)	0.065	5 (15%)	5 (29%)	0.27	4 (13%)	6 (32%)	0.15
PFKFB2	**6 (18%)**	**10 (59%)**	**0.0045***	**6 (18%)**	**10 (59%)**	**0.0045***	**6 (19%)**	**10 (53%)**	**0.027***
PFKFB3	4 (12%)	5 (29%)	0.14	**3 (9%)**	**6 (35%)**	**0.045***	**2 (6%)**	**7 (37%)**	**0.0090***
PFKFB4	8 (24%)	7 (41%)	0.21	7 (21%)	8 (47%)	0.10	**5 (16%)**	**10 (53%)**	**0.0098***
PK-L/R	3 (9%)	2 (12%)	>0.99	3 (9%)	2 (12%)	>0.99	1 (3%)	4 (21%)	0.058
PK-M2	25 (74%)	11 (65%)	0.53	24 (71%)	12 (71%)	>0.99	21 (66%)	15 (79%)	0.36
CD3	5 (15%)	2 (12%)	>0.99	3 (9%)	4 (24%)	0.20	3 (9%)	4 (21%)	0.40

Comparison made using contingency tables and Fisher's exact test

proteins (PFKFB2-4 isoforms) in this study. We also detected increased PFKFB2 and PFKFB3 in association with chronic interstitial fibrosis, which could represent sequelae of chronic rejection, other pathologies or donor factors [32]. Taken together, these results demonstrate increased glycolytic marker expression overlapping in acute tubulointerstitial inflammation and chronic injury settings.

We focussed on analysing PFK-L and associated PFKFB isoenzymes as a panel given our data and their collective role in the most important rate-limiting step of glycolysis [34]. The threshold of ≥ 3 glycolytic control proteins discriminated biopsies with TCMR compared to No TCMR with a ROC AUC of 0.73 (95% CI 0.50–0.96).

PFK-1 controls a critical step of glycolysis, which commits glucose to this metabolic pathway [34]. The PFK-L isoform is particularly concentrated in the S3 segment of the proximal tubule as well as the distal nephron, which are both located in the medulla and susceptible to changes in oxygen levels [12]. The ability of PFKFB isoenzymes to co-ordinate the formation and breakdown of fructose-2,6-bisphosphate results in tight regulation of glycolytic flux. In our study, increased expression of PFK-L in cases of TCMR was often associated with increased expression of PFKFB2-4, which are enzymes that promote the forward reaction of glycolysis. PFKFB2 is found in the kidney cortex, whereas PFKFB3 is concentrated in the medulla [12]. Although all PFKFB enzymes are hypoxia inducible, PFKFB3 has the highest kinase:phosphatase ratio of 700:1, meaning it strongly promotes the formation of fructose-2,6-bisphosphate and thus, activation of PFK-1 and the forward reaction of glycolysis [10, 34]. Notably, we observed that PFKFB4 was increased in UEV in association with TCMR and tubulitis. Although little is known about the specific role of PFKFB4 in the kidney, our group has previously observed increased UEV expression of PFKFB4 in women with pre-eclampsia [35]. We identified a threshold of ≥ 3 glycolytic control proteins as highly specific for TCMR, which highlights the collective co-ordination of the glycolytic control proteins involved in the PFK-1 step of glycolysis.

In the setting of hypoxia, tubular cells can switch from fatty acid oxidation to anaerobic glycolysis and lactate production. With injury, tubular cells may also transition to aerobic glycolysis in the presence of sufficient oxygen, known as the Warburg effect [13]. There are multiple possible reasons for increased glycolysis in TCMR. Rosenberger et al. demonstrated increased hypoxia inducible factor (HIF-1α) detection by immunohistochemistry in kidney transplant biopsies with clinical

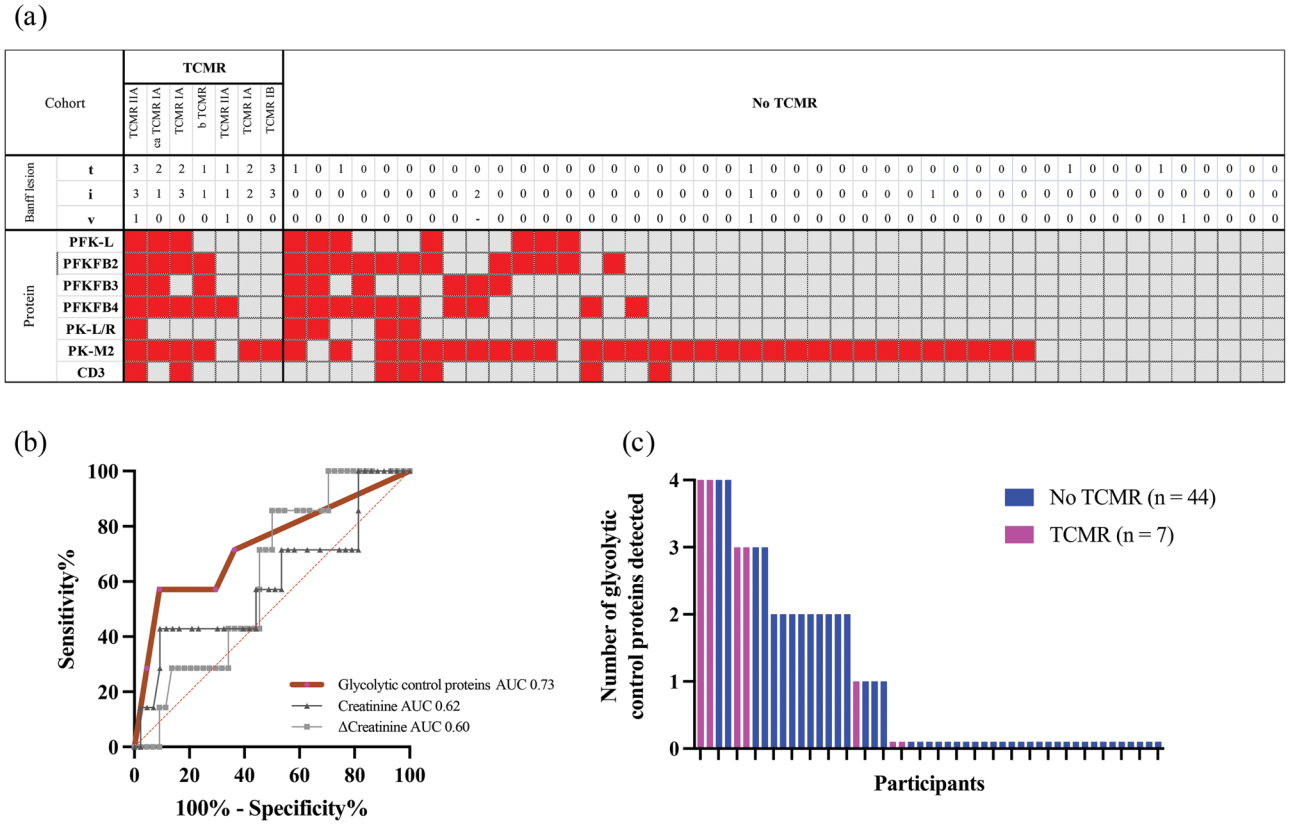

Fig. 3 (**a**) Detection of glycolytic control proteins and CD3 in TCMR (n = 7) and No TCMR (n = 44) groups. Each column represents one individual; Banff lesions t (tubulitis), i (interstitial inflammation) and v (intimal arteritis) are included. Protein detection is highlighted by red shading and absence is denoted by grey shading. TCMR, T cell-mediated rejection; caTCMR, chronic active TCMR; b TCMR, borderline TCMR. (**b**) ROC AUC analysis. ROC AUC for the panel of four glycolytic control proteins (PFK-L, PFKFB2, PFKFB3, PFKFB4) was 0.73 (95% CI 0.50–0.96). ROC AUC for creatinine at the time of indication biopsy was 0.62 (95% CI 0.43–0.81) and for Δcreatinine was 0.60 (95% CI 0.34–0.86). (**c**) Waterfall plot of the panel of four glycolytic control proteins. Each bar represents one participant (n = 51). The threshold of ≥ 3 glycolytic control proteins distinguished TCMR from No TCMR with sensitivity of 57% (95% CI 25–84) and specificity of 91% (95% CI 79–96) in this cohort with TCMR prevalence of 14%

TCMR compared to unremarkable biopsies [36]. It was postulated that this was due to increased tubular oxygen consumption in tubulitis [6]. Importantly, HIF-1α expression is known to increase expression of both PFKFB3 and PFKFB4, upregulating glycolysis [37]. Furthermore, metabolic reprogramming to aerobic glycolysis has also been demonstrated in pre-clinical models of renal fibrosis [38]. In TCMR, persistence of intra-epithelial T cells is thought to induce fibrotic transformation [38]. Therefore, increased glycolysis may be an essential repair response following immune-mediated damage to the tubular epithelium [38]. It remains uncertain whether this metabolic adaptation is beneficial or in fact exacerbates progression to fibrosis. In ischaemia-reperfusion injury, persistence of glycolytic phenotype is understood to be deleterious and to lead to chronic kidney disease [2, 39].

This study has several limitations. Firstly, whilst it is known that UEV predominantly arise from the kidney [40], it is possible that some glycolytic control proteins may be derived from EV released by intra-epithelial lymphocytes. Immune cells are known to secrete EV, which have pro- and anti-inflammatory functions [41]. Activated T cells also exhibit the Warburg effect, which is thought to be essential for T cell survival, proliferation, marker expression and cytokine release [42]. We attempted to clarify the origin of UEV by including CD3, a membrane-bound protein universally expressed by T cells and associated with the T cell receptor [43]. We did not find significantly different expression of CD3 in TCMR compared to No TCMR, which was unexpected. Park et al. utilised a magneto-electrochemical detection method for CD3 + UEV and found it was elevated in 15 patients with TCMR compared to 15 non-rejecting controls (p = 0.0008) [44]. In our study, CD3 detection in the positive control of peripheral blood mononuclear cells excluded a technical issue related to the immunoblot. It suggests that the number of T cell-derived UEV are low, compared to total UEV released from tubular epithelial cells, and that the glycolytic control proteins detected in this study were therefore predominantly from tubular cells.

Another issue is the contribution of EV from native kidneys versus kidney allografts. Oshikawa-Hori et al. demonstrated reduced aquaporin and TSG101 detection in UEV from individuals with stage 5 chronic kidney disease compared to healthy volunteers, which may indicate overall reduction of UEV released in advanced chronic kidney disease [45]. Most participants in this study (63%) received deceased donor kidney transplants, meaning these were dialysis-dependent individuals prior to transplantation, and were median time 1.8 years (IQR0.3–0.8) post-transplant at the time of study participation, reducing the likelihood of native urine output in most cases.

It is unclear whether our findings are specific for TCMR or represent a common response that may occur with other causes of tubulointerstitial injury. We observed increases in glycolytic control proteins in some cases without TCMR and have previously observed increases in UEV expression of PFKFB2-4 in pre-eclampsia [35]. It is possible that upregulation of glycolytic control proteins occurs across a broader range of tubular insults. The present study was of insufficient size to conduct subgroup analyses of TCMR group (active TCMR, chronic active TCMR, borderline TCMR) and non-rejection diagnoses such as BK virus-associated nephropathy and biopsies without significant abnormalities. Further studies in larger and more varied cohort of kidney allografts are required to address this knowledge gap. Prospective validation in an independent cohort of kidney allografts would enhance the reliability of our study findings.

In this study, one case of borderline TCMR was included in the TCMR group due to similar histopathological lesions and is often treated similarly to TCMR [46]. However, we recognise that borderline TCMR may reflect diverse immunological responses of variable clinical significance. Longitudinal studies have found that up to a third of untreated borderline TCMR progressed to TCMR [47, 48] or graft loss [49], whilst a large proportion also resolve without specific treatment. Future larger studies may enable examination of TCMR and borderline TCMR as separate entities to identify and characterise any between-group differences.

Conclusion

We detected elevations in rate-limiting enzymes of glycolysis released from kidney allografts. Particular importance of PFKFB isoenzymes was found in association with TCMR and also more broadly with tubulointerstitial inflammatory and fibrotic lesions. Glycolytic control protein expression in UEV have potential as a way to non-invasively study renal glycolysis occurring in the tubular epithelium, enabling increased understanding of allograft pathology and assessment of the health of kidney transplants.

Abbreviations

ATP	Adenosine triphosphate
DTT	Dithiothreitol
HIF-1α	Hypoxia inducible factor 1α
IQR	Inter-quartile range
NTA	Nanoparticle tracking analysis
PBS	Phosphate buffered saline
PFK-1	Phosphofructokinase-1
PFK-L	Phosphofructokinase-liver isoform
PFKFB2	Phosphofructo-2-kinase/fructose-2,6-bisphosphatase 2
PFKFB3	Phosphofructo-2-kinase/fructose-2,6-bisphosphatase 3
PFKFB4	Phosphofructo-2-kinase/fructose-2,6-bisphosphatase 4
PK	Pyruvate kinase
PK-L/R	Pyruvate kinase-L/R isoform
PK-M2	Pyruvate kinase-M2 isoform
PI	Protease inhibitor
ROC AUC	Receiver operator characteristic area under the curve
SDS	Sodium dodecyl sulfate
TCMR	T cell-mediated rejection
TSG101	Tumour susceptibility gene 101
UEV	Urinary extracellular vesicles

Supplementary Information

The online version contains supplementary material available at https://doi.org/10.1186/s12882-025-04196-y.

Supplementary Material 1

Supplementary Material 2

Acknowledgements

We thank the participants of this study.

Author contributions

PL: identification of participants and sample collection, data collection, separation of UEV, immunoblot, statistical analysis, preparation of figures and tables, initial draft of manuscript, revisions to manuscript, approval of final draft of manuscript. AG: identification of participants and sample collection, data collection, revisions to manuscript, approval of final draft of manuscript. MK: contribution to study design, sample collection, separation of UEV, immunoblot, immunoblot analysis and interpretation, revisions to manuscript, approval of final draft of manuscript. AS: blinded histopathologic examination of indication allograft biopsies together with institutional pathologists, review of allograft biopsies with missing data, revisions to manuscript, approval of final draft of manuscript. JW: supervision of the project, contribution to study design, revision to manuscript, approval of final draft of manuscript. DP: supervision of the project, initiation of study design, immunoblot analysis and interpretation, revisions to manuscript, approval of final draft of manuscript. PM: overall supervision of the project, contribution to study design, immunoblot analysis and interpretation, statistical analysis, preparation of figures and tables, revisions to manuscript, approval of final draft of manuscript, primary responsibility for final draft of manuscript. All authors read and approved the final manuscript.

Funding

PL and AG were supported by Research Training Program Scholarship from University of Melbourne. The study was also supported by funding form Austin Medical Research Fund (grant number 2-1246).

Data availability

Data is provided within the manuscript and supplementary files. Complete data set is available from the corresponding author on reasonable request.

Declarations

Ethics approval and consent to participate

This study adhered to the Declaration of Helsinki. Ethical approval was obtained from the Austin Hospital Human Research Ethics Committee

(HREC/58942/Austin-2019). Written informed consent was obtained from all participants by study investigators PL and AG.

Consent for publication
Not applicable.

Competing interests
The authors declare no competing interests.

Received: 14 January 2025 / Accepted: 19 May 2025
Published online: 06 June 2025

References

1. Li Y, Gu W, Hepokoski M, Pham H, Tham R, Kim YC, et al. Energy metabolism dysregulation in chronic kidney disease. Kidney360. 2023;4(8):1080–94.
2. Lan R, Geng H, Singha PK, Saikumar P, Bottinger EP, Weinberg JM, et al. Mitochondrial pathology and glycolytic shift during proximal tubule atrophy after ischemic AKI. J Am Soc Nephrol. 2016;27(11):3356–67.
3. Faivre A, Verissimo T, Auwerx H, Legouis D, de Seigneux S. Tubular Cell Glucose Metabolism Shift During Acute and Chronic Injuries. Front Med (Lausanne). 2021;8:742072.
4. Mårtensson J. Renal energy consumption and metabolism. Critical Care Nephrology. 2019:59–64.e1.
5. Li XB, Gu JD, Zhou QH. Review of aerobic glycolysis and its key enzymes - new targets for lung cancer therapy. Thorac Cancer. 2015;6(1):17–24.
6. Bartrons R, Simon-Molas H, Rodriguez-Garcia A, Castano E, Navarro-Sabate A, Manzano A, et al. Fructose 2,6-Bisphosphate in Cancer Cell Metabolism. Front Oncol. 2018;8:331.
7. Ross BD, Espinal J, Silva P. Glucose metabolism in renal tubular function. Kidney Int. 1986;29(1):54–67.
8. Fernandes PM, Kinkead J, McNae I, Michels PAM, Walkinshaw MD. Biochemical and transcript level differences between the three human phosphofructokinases show optimisation of each isoform for specific metabolic niches. Biochem J. 2020;477(22):4425–41.
9. Kahn A, Meienhofer M, Cottreau D, Lagrange J, Dreyfus J. Phosphofructokinase (PFK) Isozymes in Man. Human Genetics. 1979;48:93–108.
10. Rider M, Bertrant L, Vertommen D, Michels PA, Rousseau GG, Hue L. 6-Phosphofructo-2-kinase/fructose-2,6-bisphosphatase: head-to-head with a bifunctional enzyme that controls glycolysis. Biochem J. 2004;381:561–79.
11. Yi M, Ban Y, Tan Y, Xiong W, Li G, Xiang B. 6-Phosphofructo-2-kinase/fructose-2,6-biphosphatase 3 and 4: a pair of valves for fine-tuning of glucose metabolism in human cancer. Mol Metab. 2019;20:1–13.
12. Limbutara K, Chou CL, Knepper MA. Quantitative Proteomics of All 14 Renal Tubule Segments in Rat. J Am Soc Nephrol. 2020;31(6):1255–66.
13. Hardie DG. 100 years of the Warburg effect: a historical perspective. Endocr Relat Cancer. 2022;29 (12).
14. Bloom RD, Augustine JJ. Beyond the biopsy: monitoring immune status in kidney recipients. Clin J Am Soc Nephrol. 2021.
15. Nankivell BJ, Chapman JR. Histology versus molecular surveillance: claims and evidence. Kidney Int. 2023;104(3):428–32.
16. Clayton PA, McDonald SP, Russ GR, Chadban SJ. Long-term outcomes after acute rejection in kidney transplant recipients: an ANZDATA analysis. J Am Soc Nephrol. 2019;30(9):1697–707.
17. Pisitkun T, Shen RF, Knepper MA. Identification and proteomic profiling of exosomes in human urine. Proc Natl Acad Sci USA. 2004;101(36):13368–73.
18. Wu Q, Poulsen SB, Murali SK, Grimm PR, Su XT, Delpire E, et al. Large-scale proteomic assessment of urinary extracellular vesicles highlights their reliability in reflecting protein changes in the kidney. J Am Soc Nephrol. 2021;32(9):2195–209.
19. Erdbrugger U, Blijdorp CJ, Bijnsdorp IV, FE B, D B, B B, et al. Urinary extracellular vesicles: a position paper by the Urine Task Force of the International Society for Extracellular Vesicles. J Extracell Vesicles. 2021;10(7).
20. Naesens M, Roufosse C, Haas M, Lefaucheur C, Mannon RB, Adam BA, et al. The Banff 2022 kidney meeting report: reappraisal of microvascular inflammation and the role of biopsy-based transcript diagnostics. American Journal of Transplantation. 2024;24(3):338–49.
21. Thery C, Witwer KW, Aikawa E, Alcaraz MJ, Anderson JD, Andriantsitohaina R, et al. Minimal information for studies of extracellular vesicles 2018 (MISEV2018): a position statement of the International Society for Extracellular Vesicles and update of the MISEV2014 guidelines. J Extracell Vesicles. 2018;7(1):1535750.
22. Wolley MJ, Wu A, Xu S, Gordon RD, Fenton RA, Stowasser M. In primary aldosteronism, mineralocorticoids influence exosomal sodium-chloride cotransporter abundance. J Am Soc Nephrol. 2017;28(1):56–63.
23. Leung PYM, Katerelos M, Choy S, Cook N, Lee M, Paizis K, et al. Expression of NEDD4L and ENaC in urinary extracellular vesicles in pre-eclampsia. Hypertens Pregnancy. 2023;42(1):2232029.
24. Kalra H, Simpson RJ, Ji H, Aikawa E, Altevogt P, Askenase P, et al. Vesiclepedia: a compendium for extracellular vesicles with continuous community annotation. PLoS Biol. 2012;10(12).
25. DeLong E, DeLong D, Clarke-Pearson D. Comparing the areas under two or more correlated receiver operating characteristic curves: a nonparametric approach. Biometrics. 1988;44(3):837–45.
26. Welsh JA, Goberdhan DCI, O'Driscoll L, Buzas EI, Blenkiron C, Bussolati B, et al. Minimal information for studies of extracellular vesicles (MISEV2023): from basic to advanced approaches. J Extracell Vesicles. 2024;13(2).
27. Sigdel TK, Ng YW, Lee S, Nicora CD, Qian WJ, Smith RD, et al. Perturbations in the urinary exosome in transplant rejection. Front Med (Lausanne). 2014;1:57.
28. Braun F, Rinschen M, Buchner D, Bohl K, Plagmann I, Bachurski D, et al. The proteomic landscape of small urinary extracellular vesicles during kidney transplantation. J Extracell Vesicles. 2020;10(1).
29. Hoorn EJ, Pisitkun T, Zietse R, Gross P, Frokiaer J, Wang NS, et al. Prospects for urinary proteomics: exosomes as a source of urinary biomarkers. Nephrology (Carlton). 2005;10(3):283–90.
30. Lim JH, Lee CH, Kim KY, Jung HY, Choi JY, Cho JH, et al. Novel urinary exosomal biomarkers of acute T cell-mediated rejection in kidney transplant recipients: a cross-sectional study. PLoS One. 2018;13(9).
31. Jung HY, Lee CH, Choi JY, Cho JH, Park SH, Kim YL, et al. Potential urinary extracellular vesicle protein biomarkers of chronic active antibody-mediated rejection in kidney transplant recipients. J Chromatogr B Analyt Technol Biomed Life Sci. 2020;1138:121958.
32. Nankivell BJ, Shingde M, Keung KL, Fung CL, Borrows RJ, O'Connell PJ, et al. The causes, significance and consequences of inflammatory fibrosis in kidney transplantation: the Banff i-IFTA lesion. Am J Transplant. 2018;18(2):364–76.
33. Roufosse C, Simmonds N, Clahsen-van Groningen M, Haas M, Henriksen KJ, Horsfield C, et al. A 2018 Reference guide to the banff classification of renal allograft pathology. Transplantation. 2018;102(11):1795–814.
34. Mor I, Cheung EC, Vousden KH. Control of glycolysis through regulation of PFK1: old friends and recent additions. Cold Spring Harb Symp Quant Biol. 2011;76:211–16.
35. Ellis R, Katerelos M, Choy SW, Cook N, Lee M, Paizis K, et al. Increased expression and phosphorylation of 6-phosphofructo-2-kinase/fructose-2,6-bisphosphatase isoforms in urinary exosomes in pre-eclampsia. J Transl Med. 2019;17(1):60.
36. Rosenberger C, Pratschke J, Rudolph B, Heyman SN, Schindler R, Babel N, et al. Immunohistochemical detection of hypoxia-inducible factor-1alpha in human renal allograft biopsies. J Am Soc Nephrol. 2007;18(1):343–51.
37. Minchenko O, Opentanova I, Minchenko D, Ogura T, Esumi H. Hypoxia induces transcription of 6-phosphofructo-2-kinase/fructose-2,6-biphosphatase-4 gene via hypoxia-inducible factor-1alpha activation. FEBS Lett. 2004;576 (1-2).
38. Robertson H, Kirby JA. Post-transplant renal tubulitis: the recruitment, differentiation and persistence of intra-epithelial T cells. Am J Transplant. 2003;3(1):3–10.
39. Lindeman JH, Wijermars LG, Kostidis S, Mayboroda OA, Harms AC, Hankemeier T, et al. Results of an explorative clinical evaluation suggest immediate and persistent post-reperfusion metabolic paralysis drives kidney ischemia reperfusion injury. Kidney Int. 2020;98(6):1476–88.
40. Blijdorp CJ, Hartjes TA, Wei KY, van Heugten MH, Bovee DM, Budde RPJ, et al. Nephron mass determines the excretion rate of urinary extracellular vesicles. J Extracell Vesicles. 2022;11(1).
41. Buzas EI. The roles of extracellular vesicles in the immune system. Nat Rev Immunol. 2023;23(4):236–50.
42. van der Windt Gj, Pearce EL. Metabolic switching and fuel choice during T-cell differentiation and memory development. Immunol Rev. 2012;249(1):27–42.
43. Alcover A, Alarcon B, Di Bartolo V. Cell biology of T cell receptor expression and regulation. Annu Rev Immunol. 2018;16:103–25.
44. Park J, Lin HY, Assaker JP, Jeong S, Huang CH, Kurdi T, et al. Integrated kidney exosome analysis for the detection of kidney transplant rejection. ACS Nano. 2017;11(11):11041–46.

45. Oshikawa-Hori S, Yokota-Ikeda N, Sonoda H, Sasaki Y, Ikeda M. Reduced urinary release of AQP1- and AQP2-bearing extracellular vesicles in patients with advanced chronic kidney disease. Physiol Rep. 2021;9(17).
46. Loupy A, Mengel M, Haas M. Thirty years of the international banff classification for allograft pathology: the past, present, and future of kidney transplant diagnostics. Kidney Int. 2022;101(4):678–91.
47. Nankivell BJ, Chapman JR. The significance of subclinical rejection and the value of protocol biopsies. Am J Transplant. 2006;6(9):2006–12.
48. Meehan SM, Siegel CT, Aronson AJ, Bartosh SM, Thistlethwaite JR, Woodle ES, et al. The relationship of untreated borderline infiltrates by the banff criteria to acute rejection in renal allograft biopsies. J Am Soc Nephrol. 1999;10:1806–14.
49. Mehta RB, Tandukar S, Jorgensen D, Randhawa P, Sood P, Puttarajappa C, et al. Early subclinical tubulitis and interstitial inflammation in kidney transplantation have adverse clinical implications. Kidney Int. 2020;98(2):436–47.

Publisher's Note